

# Sub-Doppler laser spectroscopy on relativistic beams and tests of Lorentz invariance

C. Novotny,<sup>1</sup> G. Huber,<sup>1</sup> S. Karpuk,<sup>1</sup> S. Reinhardt,<sup>2</sup> D. Bing,<sup>2</sup> D. Schwalm,<sup>2</sup> A. Wolf,<sup>2</sup> B. Bernhardt,<sup>3</sup> T. W. Hänsch,<sup>3</sup> R. Holzwarth,<sup>3</sup> G. Saathoff,<sup>3</sup> Th. Udem,<sup>3</sup> W. Nörtershäuser,<sup>4,5</sup> G. Ewald,<sup>5</sup> C. Geppert,<sup>5</sup> T. Kühl,<sup>5</sup> T. Stöhlker,<sup>5</sup> and G. Gwinner<sup>6</sup>

<sup>1</sup>*Institut für Physik, Universität Mainz, 55128 Mainz, Germany*

<sup>2</sup>*Max-Planck-Institut für Kernphysik, 69117 Heidelberg, Germany*

<sup>3</sup>*Max-Planck-Institut für Quantenoptik, 85748 Garching, Germany*

<sup>4</sup>*Institut für Kernchemie, Universität Mainz, 55128 Mainz, Germany*

<sup>5</sup>*GSI Helmholtzzentrum für Schwerionenforschung, 64291 Darmstadt, Germany*

<sup>6</sup>*Department of Physics & Astronomy, University of Manitoba, Winnipeg, Canada R3T 2N2*

(Received 8 February 2009; revised manuscript received 18 May 2009; published 6 August 2009)

We demonstrate sub-Doppler laser spectroscopy with a beam of  ${}^7\text{Li}^+$  ions stored at 33.8% of the speed of light in the experimental storage ring at GSI. Using two lasers, the one copropagating and the other counterpropagating, with respect to the ion beam, a fluorescence line is observed via optical-optical double-resonance spectroscopy on a  $\Lambda$ -type level configuration. A linewidth of  $\approx 114$  MHz is found, which is 12 times narrower than the Doppler broadening due to the momentum spread of the ion beam. Interpreted as a test of Lorentz invariance, we find  $|\hat{\alpha}_2| < 1.2 \times 10^{-5}$ , a  $25\times$  tighter limit on  $O((v/c)^4)$  deviations from time dilation than any other experiment.

DOI: [10.1103/PhysRevA.80.022107](https://doi.org/10.1103/PhysRevA.80.022107)

PACS number(s): 03.30.+p, 41.75.Ak, 42.62.Fi

## I. INTRODUCTION

Renewed interest in experimental tests of special relativity (SR), i.e., of the underlying space-time symmetry of local Lorentz invariance, has come from one of the most salient open questions of fundamental physics—the unification of gravity with the standard model [1]. Several approaches toward quantum gravity, such as string theory [2], doubly special relativity [3], or loop quantum gravity [4] allow for small Lorentz violations. Such violations would thus provide strong experimental signatures for physics beyond the standard model.

Over the past 3 decades, laser techniques have become the method of choice for precise tests of SR. Modern implementations of the Michelson-Morley [5] and Kennedy-Thorndike [6] experiments, measuring the isotropy and velocity independence of the speed of light, make use of ultrastable lasers and optical cavities [7]. Modern Ives-Stilwell experiments [8], measuring time dilation via the Doppler shift for light emitted or absorbed from moving ions, apply high-resolution laser spectroscopy to brilliant ion beams. As first discussed by Robertson [9], these three types of experiments can be considered as the fundamental experimental corner stones of SR.

While the interferometric Michelson-Morley and Kennedy-Thorndike tests have to utilize the velocity of the earth with respect to a potential preferred frame  $\Sigma(T, \vec{X})$  [usually identified with the cosmic microwave background (CMB) rest frame with  $V_{\text{CMB}} \approx 350$  km/s  $\ll c$ ], the sensitivity of Ives-Stilwell experiments to deviations from SR can be enhanced by a large boost between the laboratory frame and the rest frame of the ion, the challenge being to maintain the precision of the measurement as the boost is increased. Using high-quality ion beams prepared in the Heidelberg test storage ring (TSR), we have recently succeeded in bringing high-precision laser spectroscopy with an absolute frequency

accuracy at the  $10^{-10}$  level to the domain of moderately fast ion beams (6.4% of the speed of light  $c$ ) and to perform the most stringent test of time dilation so far [10]. With the work reported here, we now investigate the near-relativistic regime ( $v=0.338c$ ) at the experimental storage ring (ESR) in Darmstadt and demonstrate that the quality of sub-Doppler spectroscopy on such beams can be on par with spectroscopy on slower beams. With the advent of advanced storage ring facilities [such as Facility for Antiproton and Ion Research (FAIR) at GSI], these methods will be important tools to further push time dilation tests to higher sensitivities, and at the same time they provide an experimental basis to proposals such as atomic parity violation in heavy ions at ultrarelativistic energies [11]. The current measurement at  $v=0.338c$ , although not yet in its final stage, puts already stringent limits on deviations of the time dilation relation from SR proportional to  $(v/c)^4$ .

## II. IVES-STILWELL EXPERIMENTS

In order to drive a transition of frequency  $\nu$  in an ion moving at a velocity  $\beta=v/c$  with copropagating parallel ( $p$ ) or counterpropagating antiparallel ( $a$ ) light, the frequencies  $\nu_{p,a}$  must obey the relativistic Doppler formula

$$\nu = \nu_p \gamma(1 - \beta), \quad \nu = \nu_a \gamma(1 + \beta), \quad (1)$$

where  $\gamma=(1-\beta^2)^{-1/2}$  accounts for time dilation [12]. When simultaneously driving two transitions  $\nu_1, \nu_2$  in the same ion, with a copropagating and counterpropagating laser beam, we find, independent of the ion velocity,

$$\sqrt{\frac{\nu_p \nu_a}{\nu_1 \nu_2}} = \frac{1}{\gamma(1 - \beta^2)^{1/2}} = 1. \quad (2)$$

The velocity independence of this relation is therefore a direct consequence of the unique form of the time dilation factor  $\gamma(\beta^2)$  in special relativity.

As Eq. (2) has to be valid for  $\beta=0$ , any conceivable deviation of its left-hand side from unity due to a violation of Lorentz invariance must be a function of the velocity of the ions. Moreover, as in our experiments the direction of  $\vec{\beta}$  is fixed in an earth-bound laboratory and we average over the course of a day, such a deviation cannot depend on the direction of  $\vec{\beta}$  and has to be an even function in  $\beta$ . We can thus describe possible modifications to Eq. (2) due to Lorentz violation by

$$\sqrt{\frac{\nu_p \nu_a}{\nu_1 \nu_2}} = 1 + \epsilon(\beta^2), \quad (3)$$

with  $\epsilon$  being a function of  $\beta^2$  only. For  $\beta^2 \ll 1$ , we may furthermore expand  $\epsilon(\beta^2)$  into a power series in  $\beta^2$  with expansion parameters  $\hat{\alpha}_i$ ,

$$\epsilon(\beta^2) = \hat{\alpha}_1 \beta^2 + \hat{\alpha}_2 \beta^4 + O(\beta^6). \quad (4)$$

Scenarios for the violation of Lorentz invariance are usually discussed in terms of test theories that allow for Lorentz violation but contain Lorentz symmetry as a special case. The most frequently used kinematical example of such a test model was developed by Robertson [9] and Mansouri and Sexl (RMS) [13]. Here Einstein's postulates are abolished and generalized Lorentz transformations between a hypothetical preferred reference frame  $\Sigma(T, \vec{X})$  and a frame  $S(t, \vec{x})$  moving at a velocity  $\vec{V} = \vec{\omega} \cdot c$  along  $X$  relative to  $\Sigma$  are considered, assuming an isotropic speed of light  $c$  only for  $\Sigma$ . These generalized transformations lead to modified length contraction and time dilation factors. The latter can be written as  $(\gamma_{RMS})^{-1} = (1 - \omega^2)^{1/2} \hat{a}(\omega^2)$ , where the only constraints on the function  $\hat{a}$  are: (i) it is a function of  $\omega^2$  for symmetry reasons and (ii) that  $\hat{a}(\omega^2) \rightarrow 1$  for  $\omega \rightarrow 0$ . Of course,  $\hat{a}(\omega^2) \equiv 1$  if SR holds. Following Kretzschmar [14] and Will [15], who analyzed Ives-Stilwell-type experiments within the RMS test theory, we find instead of Eq. (2),

$$\sqrt{\frac{\nu_p \nu_a}{\nu_1 \nu_2}} = \hat{a}(\beta^2), \quad (5)$$

assuming  $\beta \gg \omega (=V_{CMB}/c)$ , that is,

$$\epsilon(\beta^2) = \hat{a}(\beta^2) - 1. \quad (6)$$

Within the framework of the RMS test theory, Ives-Stilwell experiments are thus sensitive to the function  $\hat{a}$  modifying the time dilation relation of Special Relativity.

The most prominent dynamical test theory of Lorentz violation is the standard model extension (SME) [16]. Here the standard model Lagrangian is extended by Lorentz-violating terms leading to a set of test parameters for every standard model particle field. This model has triggered a wealth of Lorentz violation tests [17]. To the order  $O(\beta^2)$ , Doppler shift experiments have been analyzed in the SME and showed to be sensitive to parameter combinations in the particle sector [18] as well as in the photon sector [19]. In particular, it has been shown that within the photon sector of the SME [20], the  $O(\beta^2)$  parameter  $\hat{a}$  determined in Ives-Stilwell experiments is identical to the parameter  $\tilde{\kappa}_{Tr}$  [19], which could so far only be accessed indirectly [21,22]. It

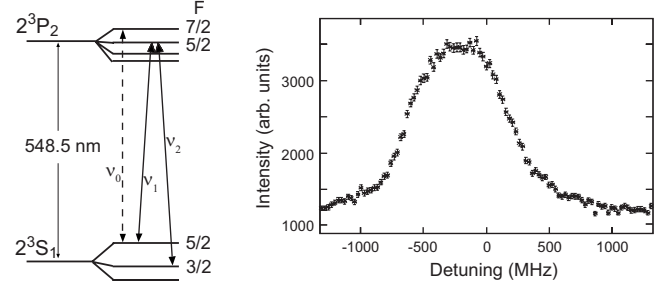


FIG. 1. Left: level scheme of the metastable  ${}^7\text{Li}^+$  ion containing a closed two-level (dashed line) and three-level ( $\Lambda$ ) system (solid lines). Right: scan across the two-level transition with the counter-propagating laser beam at  $\nu_a \sim 780$  nm.

describes isotropic Lorentz violations which most other experiments performed in the photon sector are not sensitive to as they search for sidereal variations along with the comparably small velocity of the earth through a sun-centered reference frame [7]. As this is also true for most other Lorentz tests, such as the extraordinarily sensitive clock-comparison experiments [23], the SME has only been worked out to the lowest order in  $\beta^2$  so far. In the present work, we perform an Ives-Stilwell experiment at a considerably higher velocity to take a step beyond this low-velocity limit, which will hopefully also trigger a detailed analysis of higher-order terms of  $\epsilon(\beta^2)$  in the SME.

### III. EXPERIMENTAL SETUP

In order to avoid Doppler broadening of the resonances due to the width of the ions' velocity distribution, two spectroscopy techniques have been investigated in previous Ives-Stilwell measurements at the TSR: saturation spectroscopy [10,24] and  $\Lambda$  spectroscopy [25,26]. In saturation spectroscopy, simultaneous resonance of two lasers with a transition is indicated by a Lamb dip [27] in the fluorescence spectrum. In  $\Lambda$ -type optical-optical double-resonance spectroscopy, two transitions within a closed three-level  $\Lambda$  system (see Fig. 1) are driven. With a fixed-frequency laser resonant with one of the legs of the  $\Lambda$  while scanning a second laser over the second leg, fluorescence is observed only when both lasers are resonant with the same velocity subensemble. Otherwise, the ions are pumped dark and fluorescence is suppressed. In both methods, a narrow velocity group is selected and the resulting widths of the Lamb dip or of the  $\Lambda$  resonance are free of Doppler broadening.

The moving clocks in our experiment are  ${}^7\text{Li}^+$  ions, stored at a velocity of  $0.338c$  in the ESR at GSI in Darmstadt. This He-like ion exhibits a strong optical  $2^3S_1 \leftrightarrow 2^3P_2$  transition at 548.5 nm in its metastable triplet spectrum, which is well suited for our purposes. Although the lifetime of the  $2^3S_1$  state of 50 s is quenched by collisions with the residual gas to 10–40 s, depending on the background pressure, these effective lifetimes are still long enough for beam preparation. The lifetime of the upper  $2^3P$  state of 43 ns leads to a natural linewidth of 3.7 MHz, sufficiently narrow for precision spectroscopy. Moreover, this transition can be excited with “standard” lasers aligned parallel and antiparallel to the

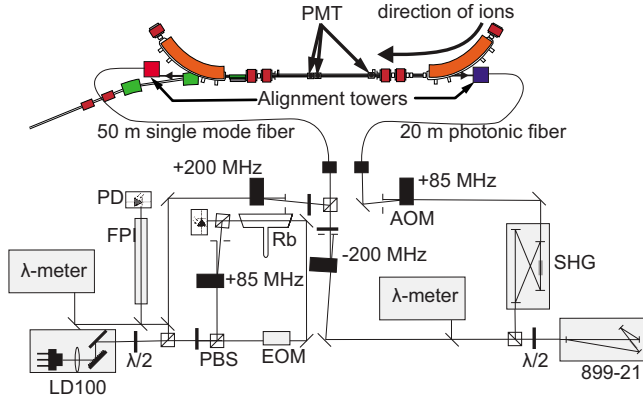


FIG. 2. (Color online) Schematic view of the experimental setup at the ESR. The laser light is provided by a laser diode (LD) and a frequency-doubled titanium sapphire laser; it is guided via fibers to the storage ring (FPI: Fabry-Perot-Interferometer; PD: photodiode; SHG: second-harmonic generation; EOM: electro-optic modulator; AOM: acousto-optic modulator).

ion beam despite of the large Doppler shifts of the transition wavelength to 386 nm and 780 nm, respectively. Finally, the selected  $^7\text{Li}^+$  line contains in its hyperfine structure a closed two-level transition  $2^3S_1(F=5/2) \leftrightarrow 2^3P_2(F=7/2)$  and a closed three-level  $\Lambda$  system  $2^3S_1(F=5/2) \leftrightarrow 2^3P_2(F=5/2)$ ,  $2^3S_1(F=3/2) \leftrightarrow 2^3P_2(F=5/2)$ , allowing for saturation and  $\Lambda$  spectroscopy, respectively (see Fig. 1).

The  $^7\text{Li}^+$  ions produced from LiF in an electron cyclotron resonance ion source are accelerated and injected into the ESR at their final energy of 58.6 MeV/u (0.338c). By minimizing the beam emittance and its longitudinal velocity spread through constant electron cooling [28], a narrow stream of clocks moving parallel at a well-defined velocity is provided. Moreover, the ion velocity can be tuned by varying the electron energy. To compensate for small energy fluctuations of the electron cooler, a weak rf signal at the tenth harmonic of the revolution frequency of the ions is applied to a pair of parallel plates. This superimposes a bunching potential copropagating with the ions that keeps them precisely at an average velocity defined by the rf frequency.

The laser setup is shown in Fig. 2. The *antiparallel* excitation of the ions is accomplished by a laser diode (Toptica DL100/LD-0780-P250-1) at 780 nm. Its frequency is calibrated with respect to the  $5S_{1/2}(F=2) \leftrightarrow 5P_{3/2}(F=3)$  line of  $^{87}\text{Rb}$ , which is known to 5.5 kHz [29], in a setup similar as described in Ref. [30]. The blueshifted light for *parallel* excitation is generated by a titanium sapphire laser (Coherent 899-21) pumped by a Coherent Verdi V18 at 532 nm; its output at 772 nm is frequency doubled in a commercial SHG unit (Tekhnoscan JS) to provide up to 280 mW at 386 nm. Alternatively, the Ti:sapphire laser can also be scanned around 780 nm to generate a second beam for antiparallel excitation. Its frequency is measured to  $\pm 100$  MHz with a commercial wave meter (Atos), which was frequently calibrated against the  $^{87}\text{Rb}$  line. The redshifted and blueshifted laser beams are chopped by acousto-optic modulators and guided to the ESR through a polarization maintaining single mode fiber (Fibercore, HB750) and a photonic crystal fiber (Crystal Fibre, LMA-PM 5), respectively.

Two alignment towers near the windows of the ESR experimental section equipped with motorized translation and rotation mirrors, as well as optical lenses, are used to align the laser beams. To optimize their (anti)parallel overlap with the ion beam, two scrapers allow to measure the positions of the ion and laser beams on both ends of the straight experimental section. Three photomultipliers (PMT) are installed along the beam tube to record the fluorescence of the excited  $\text{Li}^+$  ions around  $90^\circ$ . The PMTs are equipped with BG39 color glasses to block scattered light from the redshifted laser. Laminated long-pass filters (KV408) are added when the blueshifted laser is applied. After optimizing the spatial overlap, the ion-beam energy is fine tuned for resonance of one of the legs of the  $\Lambda$  transition with the fixed-frequency blue-shifted laser by adjusting the electron cooler voltage and the bunching frequency.

#### IV. RESULTS

The right panel of Fig. 1 shows the result of a scan of the counterpropagating laser across the closed two-level transition revealing the velocity distribution of the ion beam. The observed Doppler-broadened full width at half maximum on the order of 1 GHz reflects a well-cooled beam with  $\Delta\beta/\beta \approx 10^{-5}$ , but the line intensity reveals that less than 0.1% of the ions are in the metastable  $2^3S_1$  state. This is more than 100 times smaller than the fraction of metastable ions was increased by a stripping process in the accelerator. Note that the measured linewidth corresponds to 1.4 GHz in the rest frame of the ion, which is still a factor of  $\sim 10$  smaller than the energy difference between the hyperfine levels [31], and sufficient to ensure closed two- and three-level systems, respectively.

When shining in the blueshifted laser light, a strong increase in background counts in the photomultiplier could not be avoided despite of additional filters. Nevertheless, the resulting signal-to-noise ratio was sufficient for  $\Lambda$  spectroscopy. To investigate its shape, we first recorded the  $\Lambda$  resonance with two lasers at  $\sim 780$  nm, both counterpropagating with respect to the ion beam—thereby avoiding the additional background. By scanning only one laser and keeping the other one's frequency fixed, we recorded a clear sub-Doppler  $\Lambda$  resonance as shown in Fig. 3(a). From a Lorentzian fit, a linewidth of approximately 80 MHz is obtained, corresponding to 114 MHz in the ions' rest frame. This is comparable to the linewidths observed at the TSR for  $\Lambda$  spectroscopy [26], but still broader than typical Lamb dips observed in saturation spectroscopy. The additional broadening of the  $\Lambda$  resonance is mainly caused by a memory effect of the revolving ions; velocity-changing collisions of ions that were previously pumped dark can bring them back into resonance even if the lasers are detuned from resonance. These velocity changes, which occur over many roundtrips of the ions in the storage ring, may also lead to a net frequency shift, if they are asymmetric with respect to the design velocity  $\beta_0$ , e.g., for an ion beam that is gradually slowed down during the scan. In our experiment, however, the mean ion velocity is fixed by ion-beam bunching, which



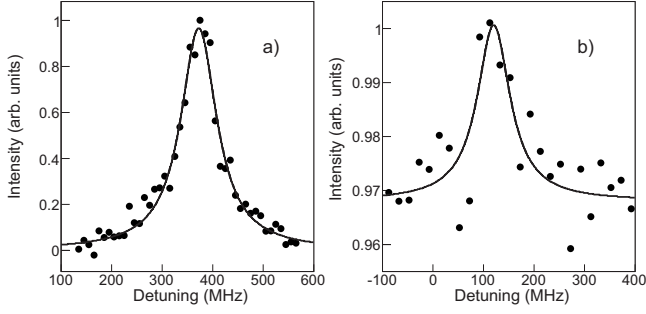


FIG. 3.  $\Lambda$  resonances versus detuning of the scanning diode laser observed (a) with both lasers counterpropagating and (b) with one copropagating and one counterpropagating laser with respect to the ion beam. The solid lines represent Lorentz fits.

forces the ions into synchrotron oscillations around  $\beta_0$ . Since the true resonance position must be within the frequency range, where a  $\Lambda$  fluorescence signal is observed, we conservatively estimate the frequency uncertainty due to the velocity changes as smaller than the linewidth, which corresponds to  $\pm 40$  MHz in the present case. In future experiments, a main part of the contribution of the memory effect to the  $\Lambda$  signal will be measured and subtracted with a method developed at the TSR [26]. This will significantly reduce the influence of velocity-changing collisions on the  $\Lambda$  resonance width.

A sensitive test of time dilation requires copropagating and counterpropagating laser beams. The corresponding  $\Lambda$  resonance obtained with a fixed-frequency blueshifted laser and a scanning redshifted laser is plotted versus the frequency detuning from the  $^{87}\text{Rb}$  line in Fig. 3(b). The signal-to-noise ratio is sufficient to determine the center  $\nu_a$  of the  $\Lambda$  resonance to an accuracy of 48 MHz, which includes the fit uncertainty of 11 MHz, 40 MHz from the memory effect, and 25 MHz due to systematic uncertainties caused by the alignment of the laser beams, their Gaussian phase structure, and ion-beam properties. The 100 MHz accuracy of the wave meter limits the accuracy of the blueshifted laser frequency  $\nu_p$  to 200 MHz. A further systematic uncertainty may be caused by the magnetic fields in the ESR experimental section. Despite the use of linearly polarized light, the Zeeman effect might not only cause symmetric broadening but also a net frequency shift when the ion beam becomes polarized by optical pumping [10]. However, for the fields present near the photomultiplier, this shift is estimated to be below 5 MHz and can be neglected at the present level of accuracy. A summary of the relevant frequencies is given in Table I. The measured Doppler shifts are consistent with SR; applying

TABLE I. Rest-frame frequencies  $\nu_1$  and  $\nu_2$  of the  $\Lambda$  transition and corresponding Doppler-shifted frequencies  $\nu_a$  and  $\nu_p$  observed with counterpropagating laser beams (in MHz).

$\nu_1$ ( $F=5/2 \leftrightarrow F=5/2$ ) <sup>a</sup>	$546455144.8 \pm 0.4$
$\nu_2$ ( $F=3/2 \leftrightarrow F=5/2$ ) <sup>a</sup>	$546474962.7 \pm 0.4$
$\nu_p$	$777204676 \pm 200$
$\nu_a$	$384228270 \pm 48$

<sup>a</sup>Reference [32].

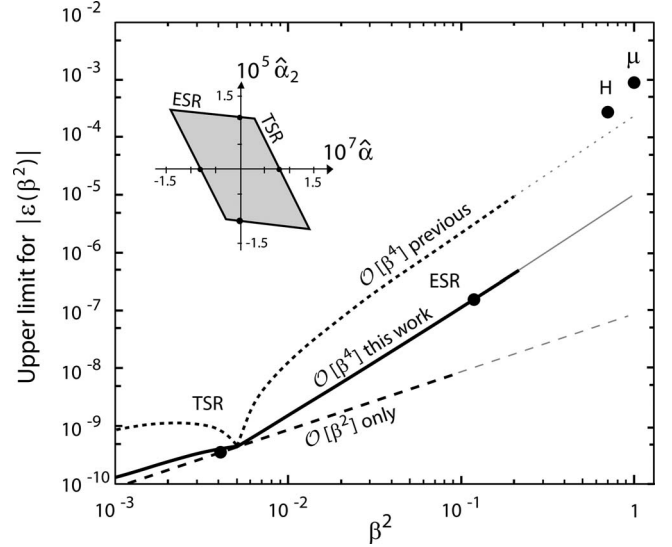


FIG. 4. Upper limits for deviations of high velocity Ives-Stilwell experiments from the prediction of SR as a function of  $\beta^2$ . The solid dots are limits for  $|\epsilon(\beta^2)|$  deduced in previous experiments at the TSR [10,24] and in the present investigation at the ESR. The dashed and dotted curves are limits obtained from previous results when including terms of up to the order  $O(\beta^2)$  and  $O(\beta^4)$ , respectively, in the expansion of  $\epsilon(\beta^2)$  [see Eq. (4)]. The thick solid line is the limit implied by combining the TSR result with the result of the present measurement; the resulting restriction for the expansion parameters  $\hat{\alpha}$  and  $\hat{\alpha}_2$  are shown in the inset. The limits marked by H and  $\mu$  are obtained from a Doppler shift experiment on H [33] and a lifetime measurement of the muon [34] when interpreting  $\epsilon(\beta^2)$  within the RMS test theory.

Eq. (3) we find an upper bound for possible deviations from SR at  $\beta=0.338$  of

$$|\epsilon(\beta^2)| < 1.5 \times 10^{-7}. \quad (7)$$

## V. DISCUSSION AND OUTLOOK

Due to the high ion velocity, the result is a significant step to further limit the function  $\epsilon(\beta^2)$ . The TSR experiments were performed at two velocities ( $\beta_1=0.03$  and  $\beta_2=0.064$ ) and interpreted by considering only the order  $O(\beta^2)$  term in the expansion of  $\epsilon(\beta^2)$  [see Eq. (4)] to be relevant, implying the tacit assumption usually made in this field that “reasonable” higher-order expansion parameters  $\hat{\alpha}_i$  are only on the order of  $\hat{\alpha}$  or less. This analysis resulted in [10]  $|\hat{\alpha}| < 8.4 \times 10^{-8}$  (dashed line in Fig. 4).

Allowing also  $\hat{\alpha}_2 \neq 0$  without any *ad hoc* assumptions about its size, the TSR experiments alone led to an upper limit for  $|\epsilon(\beta^2)|$  as indicated by the dotted line in Fig. 4. Combining the TSR and the ESR results, one obtains a new limit for  $|\epsilon(\beta^2)|$  as shown by the thick solid line in Fig. 4: an up to  $25\times$  improvement over the previous restriction. The allowed parameter space for  $\hat{\alpha}$  and  $\hat{\alpha}_2$  is shown in the inset of Fig. 4 and implies

$$|\hat{a}_2| < 1.2 \times 10^{-5}.$$

Interpreting the Ives-Stilwell experiments within the framework of the RMS test theory,  $\epsilon(\beta^2)$  is connected to the function  $\hat{a}(\beta^2)$ , modifying the SR time dilation by Eq. (6). Within this framework, the present result can also be compared to upper limits for  $\hat{a}(\beta^2)$  deduced from a Doppler shift measurement on hydrogen at  $\beta=0.84$  [33] and from a measurement of the muon lifetime [34] at  $\beta=0.9994$ . As shown in Fig. 4, the present limit on  $\hat{a}_2$  is up to almost two orders of magnitude more stringent than those implied by these previous ultrahigh velocity experiments.

In summary, the present investigation demonstrates that sub-Doppler spectroscopy can be performed with relativistic ion beams using the Ives-Stilwell geometry. For  $\Lambda$  spectroscopy, linewidths have been reached, which are comparable to those observed at lower velocities at the TSR [26], and we

are confident that in saturation spectroscopy, linewidths on the order of the natural linewidths ( $\sim 10$  MHz) can be achieved as in previous TSR experiments [10] once the background problem caused by the blueshifted laser has been solved. The latter is presently under detailed investigation. Together with a more precise frequency determination of the blueshifted laser, we expect to be able to further improve the present limit for  $|\epsilon(\beta^2)|$  at  $\beta=0.338$  by up to two orders of magnitude.

## ACKNOWLEDGMENTS

We gratefully acknowledge M. Steck, F. Nolden, and K. Tinschert for technical support and F. Bosch and H.-J. Kluge for helpful discussions. T.W.H. gratefully acknowledges support by the Max-Planck Foundation. This work was supported by the Helmholtz Association under Contract No. VH-NG-148.

- 
- [1] D. Mattingly, *Living Rev. Relativ.* **8**, 5 (2005).
  - [2] V. A. Kostelecký and S. Samuel, *Phys. Rev. D* **39**, 683 (1989).
  - [3] G. Amelino-Camelia, *Nature (London)* **418**, 34 (2002).
  - [4] R. Gambini and J. Pullin, *Phys. Rev. D* **59**, 124021 (1999).
  - [5] A. A. Michelson and E. H. Morley, *Am. J. Sci.* **34**, 333 (1887).
  - [6] R. J. Kennedy and E. M. Thorndike, *Phys. Rev.* **42**, 400 (1932).
  - [7] P. Antonini, M. Okhapkin, E. Goklu, and S. Schiller, *Phys. Rev. A* **71**, 050101(R) (2005); H. Müller, P. L. Stanwix, M. E. Tobar, E. Ivanov, P. Wolf, S. Herrmann, A. Senger, E. Kovalchuk, and A. Peters, *Phys. Rev. Lett.* **99**, 050401 (2007).
  - [8] H. E. Ives and G. R. Stilwell, *J. Opt. Soc. Am.* **28**, 215 (1938).
  - [9] H. P. Robertson, *Rev. Mod. Phys.* **21**, 378 (1949).
  - [10] S. Reinhardt *et al.*, *Nat. Phys.* **3**, 861 (2007).
  - [11] M. Zolotarev and D. Budker, *Phys. Rev. Lett.* **78**, 4717 (1997).
  - [12] A. Einstein, *Ann. Phys.* **322**, 891 (1905).
  - [13] R. Mansouri and R. U. Sexl, *Gen. Relativ. Gravit.* **8**, 497 (1977).
  - [14] M. Kretzschmar, *Z. Phys. A* **342**, 463 (1992).
  - [15] C. M. Will, *Phys. Rev. D* **45**, 403 (1992); the function  $a(\omega^2)$  defined by Will is connected with the corresponding function  $\hat{a}(\omega^2)$  by  $a(\omega^2)=(1-\omega^2)^{1/2}\hat{a}(\omega^2)$ .
  - [16] D. Colladay and V. A. Kostelecký, *Phys. Rev. D* **58**, 116002 (1998).
  - [17] *CPT and Lorentz Symmetry IV*, edited by V. A. Kostelecký (World Scientific, Singapore, 2008); A. Kostelecký and N. Russell, e-print arXiv:0801.0287.
  - [18] C. D. Lane, *Phys. Rev. D* **72**, 016005 (2005).
  - [19] M. E. Tobar, P. Wolf, A. Fowler, and J. G. Hartnett, *Phys. Rev. D* **71**, 025004 (2005); M. Hohensee, A. Glenday, C. H. Li, M. E. Tobar, and P. Wolf, *ibid.* **75**, 049902(E) (2007).
  - [20] V. A. Kostelecký and M. Mewes, *Phys. Rev. D* **66**, 056005 (2002).
  - [21] F. R. Klinkhamer and M. Schreck, *Phys. Rev. D* **78**, 085026 (2008).
  - [22] M. A. Hohensee, R. Lehnert, D. F. Phillips, and R. L. Walsworth, *Phys. Rev. Lett.* **102**, 170402 (2009).
  - [23] F. Canè, D. Bear, D. F. Phillips, M. S. Rosen, C. L. Smallwood, R. E. Stoner, R. L. Walsworth, and V. A. Kostelecký, *Phys. Rev. Lett.* **93**, 230801 (2004).
  - [24] G. Saathoff, S. Karpuk, U. Eisenbarth, G. Huber, S. Krohn, R. Muñoz Horta, S. Reinhardt, D. Schwalm, A. Wolf, and G. Gwinner, *Phys. Rev. Lett.* **91**, 190403 (2003).
  - [25] R. Grieser *et al.*, *Appl. Phys. B: Lasers Opt.* **59**, 127 (1994).
  - [26] G. Saathoff *et al.*, *Lect. Notes Phys.* **702**, 479492 (2006).
  - [27] W. E. Lamb, *Phys. Rev.* **134**, A1429 (1964).
  - [28] M. Steck *et al.*, *Nucl. Instrum. Methods Phys. Res. A* **532**, 357 (2004).
  - [29] J. Ye *et al.*, *Opt. Lett.* **21**, 1280 (1996).
  - [30] S. Reinhardt *et al.*, *Opt. Commun.* **261**, 282 (2006).
  - [31] J. J. Clarke and W. A. van Wijngaarden, *Phys. Rev. A* **67**, 012506 (2003).
  - [32] E. Riis, A. G. Sinclair, O. Poulsen, G. W. F. Drake, W. R. C. Rowley, and A. P. Levick, *Phys. Rev. A* **49**, 207 (1994).
  - [33] D. W. MacArthur, K. B. Butterfield, D. A. Clark, J. B. Donahue, P. A. M. Gram, H. C. Bryant, C. J. Harvey, W. W. Smith, and G. Comtet, *Phys. Rev. Lett.* **56**, 282 (1986).
  - [34] J. Bailey *et al.*, *Nature (London)* **268**, 301 (1977).